CHEMISTRY OF MATERIALS

Article

pubs.acs.org/cm

Method for Manufacturing Membranes with Ultrathin Hydrogel Selective Layers for Protein Purification: Interfacially Initiated Free Radical Polymerization (IIFRP)

Ilin Sadeghi, Hyunmin Yi, and Ayse Asatekin*

Chemical and Biological Engineering Department, Tufts University, Medford, Massachusetts 02155, United States

Supporting Information

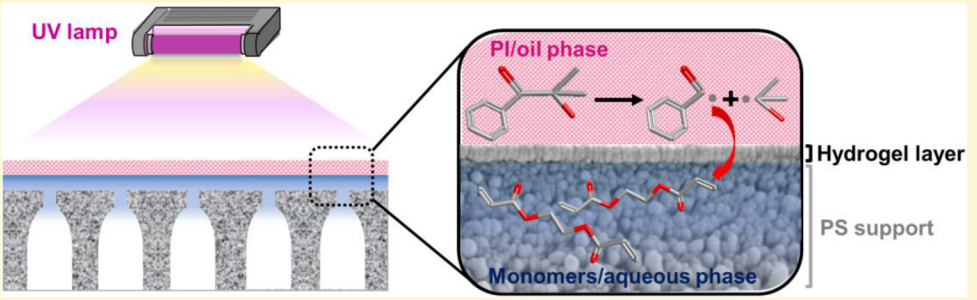

ABSTRACT: Hydrogels are promising materials as membrane selective layers due to their fouling-resistant nature, tunable mesh size, and functionalizability. These features are especially critical for protein purification applications. However, the fabrication of thin, uniform hydrogel membrane selective layers using a simple, scalable process is an unmet challenge. We demonstrate a new method, interfacially initiated free radical polymerization (IIFRP), for fabrication of ultrathin hydrogel selective layers on porous supports in a simple and reproducible process. This method utilizes segregation of the monomer and the photoinitiator into two separate, immiscible phases to form a very thin, uniform, and defect-free hydrogel layer at the interface upon photopolymerization. The resulting hydrogel-coated membranes have selective layers as thin as <100 nm, and can separate the proteins based on their size with a sharp molecular weight cutoff. The method is readily tunable for a broader range of separations simply by altering experimental parameters (e.g., UV exposure time, monomer concentration) or addition of inert porogens/comonomers. Membranes prepared using this method exhibit extremely high antifouling properties upon extended exposure to protein solution providing a promising approach for protein purification. Taken together, these findings illustrate a significant step toward simple, robust, and scalable fabrication of ultrathin, functional hydrogel selective layers in a controlled manner, with potential applications in bioseparations, wastewater treatment, and gas separation.

INTRODUCTION

Protein purification is of great importance in a wide range of applications including the pharmaceutical, biotechnology, cosmetics, and food industries as well as in enzymatic catalysis.[1,2] Membrane separation processes are attractive for these applications due to their high throughput, ease of implementation, and cost effectiveness.[3,4] However, critical challenges remain in the use of membranes for protein purification. First, protein separations require membranes with well-controlled selectivity.[5−8] Second, fouling due to the adsorption of the proteins and other biomolecules in the feed leads to substantial decline in membrane permeance and lifetime,[9,10] and can cause shifts in membrane pore size.[9,11,12] Addressing these concerns can broaden the use of membrane processes in the manufacture and purification of biopharmaceuticals.

Hydrogels are especially promising materials for membranes targeted at protein purification, because they are effective, versatile, tunable, functionalizable, and inherently fouling-resistant.[13] Selectivity can be controlled by the mesh size of the cross-linked polymer, with effective pore sizes typically in the ultrafiltration (UF) range (1−5 nm), suitable for protein purification.[14] Functional groups can be easily integrated into these selective layers, enabling more targeted control of membrane selectivity and broadening their potential applications to protein separations. Moreover, hydrogels are inherently hydrophilic, which makes them very fouling-resistant.[15−18] Despite these promising features, if the hydrogel will serve as the selective layer of a membrane, it has to be as thin as possible, because membrane flux is inversely proportional to the layer thickness. However, the fabrication of hydrogels as thin, defect-free membrane selective layers remains a major challenge.

Existing literature on hydrogel membranes focuses mainly on free-standing films.[14,17,19,20] These hydrogel films are prepared by dissolving the monomer and initiator in an aqueous solution,

Received: November 2, 2017
Revised: February 2, 2018
Published: February 3, 2018

DOI: 10.1021/acs.chemmater.7b04598
Chem. Mater. XXXX, XXX, XXX−XXX

Scheme 1. Schematic Showing Fabrication[a] of Membranes with Ultrathin Hydrogel Selective Layers by Interfacially Initiated Free Radical Polymerization (IIFRP)

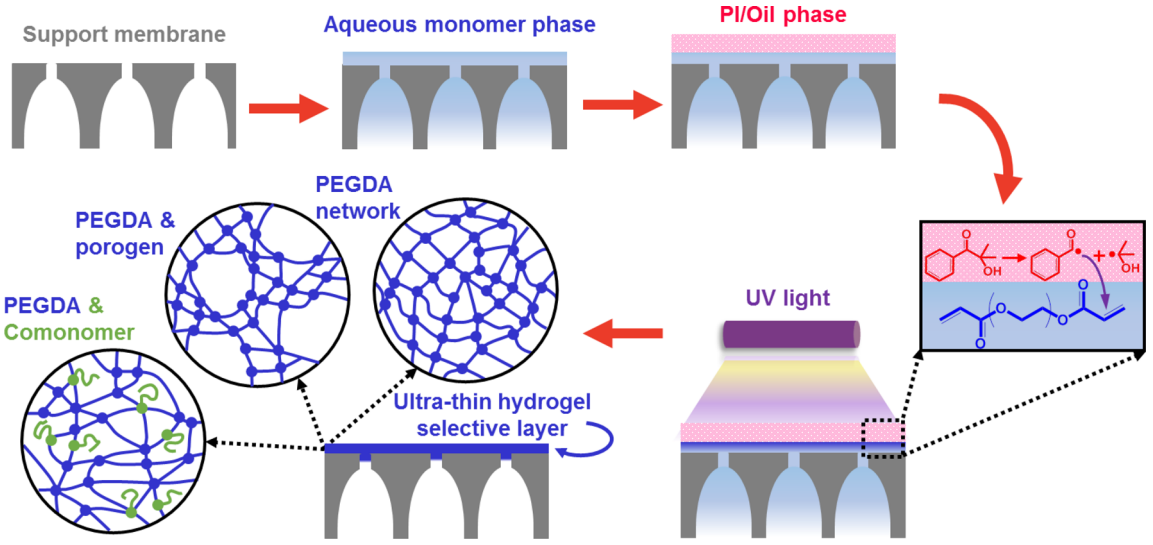

[a]A porous support membrane is immersed in an aqueous monomer solution, which fills its pores and leaves a thin layer on its surface. The membrane is then covered with an oil phase containing a photoinitiator (PI), and irradiated with UV light. The hydrophobic photoinitiator dissociates and reacts with the aqueous monomer at the interface, forming a thin hydrogel layer covering the support. The monomer solution can contain PEGDA with or without porogens or comonomers, which can alter layer permeability and control selectivity.

spreading this mixture into a thin layer, and initiating polymerization, typically by UV illumination. This results in the formation of a very thick hydrogel layer (100−900 μm), and the resultant membranes have very low flux. To decrease film thickness while maintaining mechanical integrity, 1−10 μm hydrogel layers can be formed on porous supports by carefully designed coating methods.[13,21] However, this approach requires a high-viscosity monomer solution and specific wetting properties to achieve a good coating that remains on top of the membrane. The viscosity can be increased with additives (e.g., high-molecular-weight inert polymers),[16] but this can simultaneously change coating properties such as pore size.[16,22,23] Another surface modification approach, grafting[13,24] from the membrane surface, creates a polymer brush lining the membrane pores and surface rather than a continuous selective layer.[24,25] To form a selective layer by grafting, the pore diameter has to be spanned by growing polymer chains from a limited number of initiating sites on pores followed by cross-linking. This can require long reaction times and is prone to defects due to pore size polydispersity in the support membrane. Thus, there is a critical need for a simple and reproducible fabrication method that enables the formation of a very thin, defect-free hydrogel selective layer using processes that can be easily integrated into large-scale manufacturing schemes. Such a method would enable the development of a wide range of membrane materials not only for protein purification, but also for wastewater treatment[16,26] and gas separation applications.[27,28]

The most common method for the large-scale fabrication of membranes with ultrathin selective layers is interfacial polymerization (IP).[29,30] Thin film composite (TFC) membranes fabricated using this method feature a very thin selective layer (typically <100 nm) on a porous support that provides mechanical integrity.[31−33] IP involves the polymerization of two highly reactive monomers segregated in two immiscible phases (i.e., a diamine in aqueous solution and a diacyl chloride in an organic phase). The polymer forms as a thin film at the interface of the two phases covering the surface of the porous support. Although this method is established, simple, and scalable to a roll-to-roll process, it is limited to a narrow range of polymer chemistries that are formed by condensation polymerization. IP cannot be applied to polymers prepared by free radical polymerization (FRP) such as hydrogels. It also cannot be used to fabricate inherently hydrophilic layers, because one of the monomers has to be oil-soluble. Furthermore, IP also generates a highly cross-linked and dense layer that limits the application of this method to desalination and reverse osmosis (RO). Larger pore sizes suitable for protein purification are typically not easily accessible.

Our approach to addressing these challenges centers on a novel, scalable, and robust fabrication method inspired by IP, called interfacially initiated free radical polymerization (IIFRP). The novelty of this approach arises from its ability to create ultrathin, fully hydrophilic selective layers from a wide range of water-soluble monomers that propagate by free radical polymerization (e.g., acrylates, methacrylates, acrylamides). In IIFRP, as illustrated in Scheme 1, the monomer(s) and initiator are segregated into two immiscible phases: an aqueous monomer, and an organic/oil phase containing photoinitiator. The support membrane is first immersed in the aqueous monomer solution, which fills its pores and leaves a thin layer on its surface. The organic/oil layer containing an oil-soluble photoinitiator is then added to cover the top of the membrane. Upon irradiation with a UV lamp, a uniform and thin hydrogel layer is formed at the oil−water interface spanning the surface of the support membrane. Limited solubility of the initiator in the monomer layer, and the interfacial tension between the aqueous and oil layers creates a uniform, continuous, defect-free selective layer at the interface.

This report is the first demonstration of this new, simple, scalable, reliable, and robust technique for manufacturing membranes with ultrathin, defect-free hydrogel selective layers. We first show that IIFRP can be used to create layers as thin as

DOI: 10.1021/acs.chemmater.7b04598
Chem. Mater. XXXX, XXX, XXX−XXX

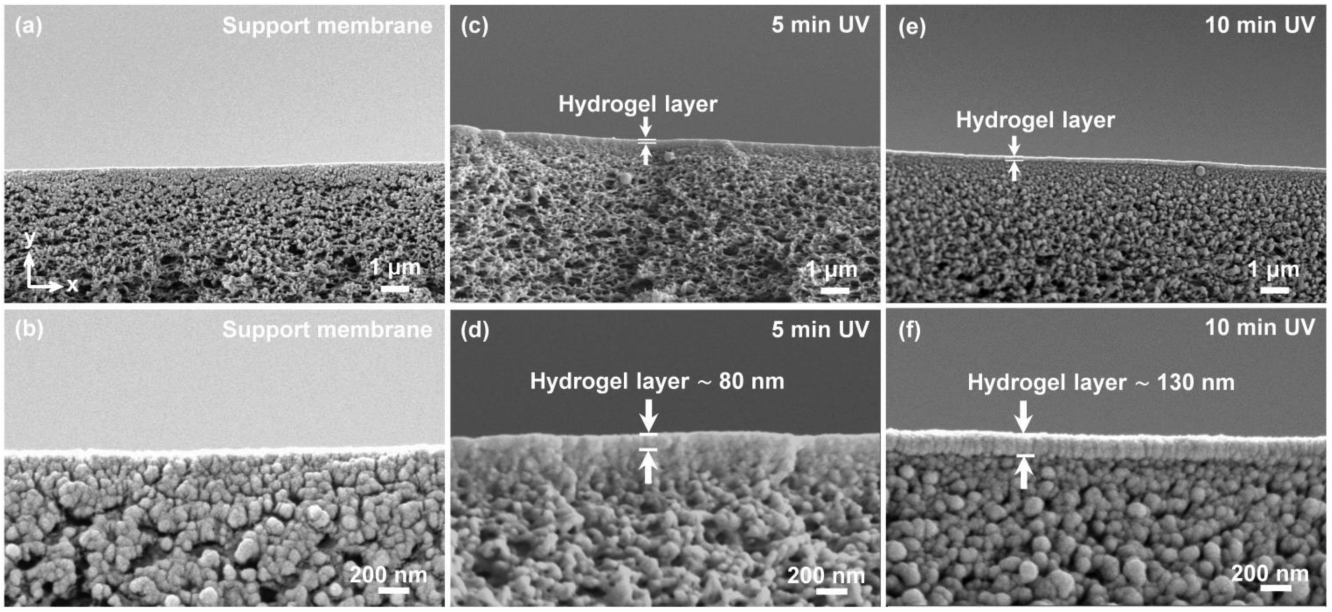

Figure 1. Morphology of (a) support membrane, PS. (b) Higher magnification of PS support. (c) Hydrogel layer at 5 min UV exposure time. (d) Higher magnification of hydrogel at 5 min UV exposure time. (e) Hydrogel layer after 10 min UV exposure time. (f) Hydrogel layer at 10 min UV exposure time at higher magnification. Continuous and uniform hydrogel layers are formed on the support membrane upon exposure to UV at varying times. Longer UV exposure time leads to formation of a thicker layer.

<100 nm on commercially available porous supports. We then show that the permeance and pore size of selective layers formed by our method can be readily altered through simple parameters (e.g., monomer concentration, UV exposure time) or through the addition of comonomers or inert polymers in the monomer solution. Finally, we demonstrate the stability and extremely high fouling resistance of the hydrogel layer in filtering protein solutions. We envision that this new technique, IIFRP, could serve as a platform for manufacturing membranes with a broad range of properties (e.g., selectivity, affinity) for several applications beyond protein purification, such as wastewater treatment, natural gas upgrading, and water purification.

■ RESULTS AND DISCUSSION

Hydrogel Layer Morphology. As the first demonstration of the IIFRP method to manufacture membranes with hydrogel selective layers, we first immersed a commercial UF membrane (PS35, Nanostone), which will act as the porous support, into an aqueous solution containing the poly(ethylene glycol) diacrylate (PEGDA) monomer. In most cases, we added an inert hydrophilic polymer, poly(ethylene glycol) with an average molar mass of 200 g mol^{-1}, PEG200, as an additive. The selection was based on the previous literature stating that inert short-chain PEG can create a porous network,[34−36] which in turn would be expected to lead to an increase in membrane permeance. The effect of additives on membrane permeance and selectivity is further discussed in the following section. Next, we removed the support from the aqueous solution, dabbed off the excess, and covered it with the oil solution, *n*-hexadecane containing 0.1% v/v of the hydrophobic photoinitiator (PI), Darocur 1173. We then exposed it to UV light, which caused the initiator to form free radicals in the oil phase that then diffused to the aqueous phase and started the polymerization of PEGDA (Scheme 1). The membrane surface was covered by a glass plate during UV exposure to prevent initiation from PS support membrane upon exposing to UV light, as reported in previous studies.[37,38] A control experiment performed without the addition of PI into the oil phase did not lead to a significant change in permeance.

Our approach, IIFRP, is in direct contrast to the established photoinitiated free radical polymerization (FRP) methods for preparing hydrogel layers, where monomers and PI are both in the aqueous phase. Using this method, a solution containing only the monomer and the PI cannot typically be coated onto a porous support. The solution is instantly absorbed into the membrane pores through capillary action, and the whole support is filled with hydrogel. Indeed, when the above procedure was performed using a monomer solution containing a water-soluble initiator, this was the result (Supporting Information). The viscosity of the solution can sometimes be increased by increasing the concentration of the solution (Figure S1, Supporting Information) or adding high-molecular-weight polymers,[16] but this often results in the formation of a very thick layer and changes the resultant membrane properties. Furthermore, the uneven exposure to UV light and polymerization-induced phase separation (PIPS) can lead to macroscale porosity in the film.[19,39]

In contrast, IIFRP segregates the reactants (i.e., monomers and PI) into two separate phases. Free radicals formed by PI upon UV exposure diffuse to the oil−water interface and react with the monomers in the aqueous monomer solution to initiate polymerization. Since the PI is insoluble in water, the polymer layer starts forming at and growing from the oil−water interface. When UV irradiation is stopped, the polymerization process also ends, arresting the growth of the selective layer. Thus, longer UV irradiation times are expected to result in thicker selective layers. This would not necessarily be the case for homogeneous FRP, where longer exposure would likely increase the degree of cross-linking but not necessarily the coating thickness once the gel point is reached. It is also in contrast to traditional IP, where the formation of the highly cross-linked selective layer at the interface hinders the diffusion of the monomers, leading to a self-limiting reaction. The mesh

DOI: 10.1021/acs.chemmater.7b04598
Chem. Mater. XXXX, XXX, XXX−XXX

size of the hydrogel layer that forms in IIFRP is much larger in comparison to the monomer size. This means monomers easily diffuse to the interface and react with the initiating radicals, enabling the hydrogel layer to build as long as radicals are generated through UV irradiation.

To test this hypothesis, we prepared membranes with varying UV irradiation times and analyzed the resultant membrane morphology by field-emission scanning electron microscopy (FESEM). Figure 1a,b shows the commercial polysulfone (PS) membrane with nominal molecular weight cutoff (MWCO) of 20 kDa that we utilized as the porous support throughout the study. Typical of asymmetric ultrafiltration membranes, the membrane has smaller pores on top and larger macrovoids in the sublayers. When IIFRP was applied to this support membrane using 5% v/v PEGDA as the monomer solution and a UV exposure time of 5 min, a very thin hydrogel coating layer was formed (Figure 1c,d). The higher-magnification image of this membrane (Figure 1d) shows the presence of the layer more clearly. The layer is well-integrated into the support, penetrating slightly below the top surface pores and anchoring into the support as envisioned. This morphology prevents the delamination of the layer, but also makes it difficult to clearly identify the boundaries of this layer and determine the thickness. To further confirm the evenness and uniformity of the hydrogel layer formed on the support membrane, we dissolved the support layer in dichloromethane and transferred the hydrogel layer to a wire lasso (Figure S2, Supporting Information). Although, the layer is very thin, it formed an integral surface across the whole 1 cm diameter of the lasso, providing solid evidence of the uniform and continuous nature of the hydrogel layer.

When IIFRP was performed using 10 min UV exposure under identical conditions, a more distinct layer is formed compared with the shorter irradiation time of 5 min (Figure 1e,f). Notably, the layer appears to be uniform throughout the membrane imaged along the *x*-direction labeled in the figure. This uniform layer is maintained throughout the entire membrane sample, imaged in different frames sampling the length of the sample (data not shown), clearly indicating the consistent nature of this simple method. A higher-magnification image of this membrane (Figure 1f) shows that the layer is also uniform across the layer thickness (*y*-direction). The coating is thicker and more distinct in this sample compared to 5 min UV exposure time, allowing a rough estimation of the thickness to be around 130 nm. Longer UV exposure appears to increase the dry thickness of the hydrogel layer. For example, an even longer exposure time of 20 min led to the formation of a hydrogel layer with thickness of 260 nm, about twice the one formed at 10 min UV exposure time (Figure S3, Supporting Information). Accounting for the uniform thickness of the aqueous prepolymer layer during the polymerization and the status of the membrane sample during SEM imaging (i.e., dried), the observed difference in the thickness is likely due to the polymerization process penetrating into the membrane to different extents. Importantly, this result suggests that simple fabrication parameters such as UV irradiation time can be used to impart various membrane properties (e.g., layer thickness and penetration).

Chemical Structure of the Hydrogel Layer. In order to further confirm the formation of the ultrathin hydrogel layers, we performed attenuated total reflection−Fourier transform infrared spectroscopy (ATR−FTIR) on membranes prepared by IIFRP using a monomer solution containing 5% v/v PEGDA, 2.5% v/v PEG200, and a UV exposure of 5 min (Figure 2). PEGDA (Figure 2a) forms a cross-linked PEGDA

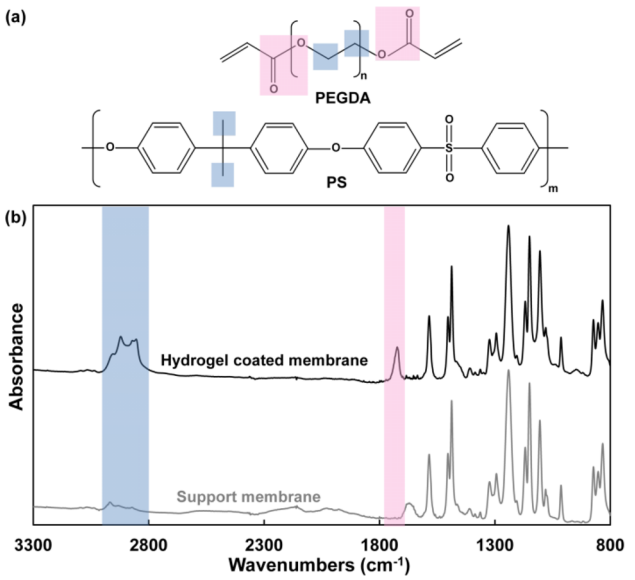

Figure 2. (a) Chemical structure of PEGDA and PS. (b) ATR−FTIR spectra of PS support membrane (bottom) and coated with an ultrathin hydrogel layer (top) with 5 min UV exposure. Absorption bands corresponding to CH (blue) and ester (pink) groups are marked to demonstrate the formation of a cross-linked PEGDA hydrogel selective layer in the PS support.

network upon photoinduced free radical polymerization on the membrane surface. This leads to an increase in the density of C−H bonds (blue) in comparison with the support membrane material PS, and also introduces ester groups (pink).

Indeed, upon the deposition of the cross-linked PEGDA selective layer by IIFRP, the broad absorbance peak around 2800−3000 cm^{-1} (top spectrum) corresponding to the C—H stretching vibration increases in intensity.[40,41] This peak is very weak in the support membrane (bottom spectrum), which does not contain as high a concentration of C—H groups (labeled blue in Figure 2). This clearly confirms the presence of the PEG hydrogel layer. The presence and chemical structure of the coating layer is also confirmed by the appearance of the C═O stretching peak at 1723 cm^{-1} arising from the ester bond at each end of the PEGDA (labeled pink),[40] while the IR spectrum of the support membrane (bottom) shows no such peak.

In addition, the coating shows no significant absorbance at 1620−1640 cm^{-1}. This wavelength range corresponds to the vinyl groups in PEGDA that are converted to single bonds upon polymerization.[40] The lack of a peak in this range in the spectrum of the coated membrane suggests that the formed hydrogel layer is mostly or fully polymerized, mostly free of unpolymerized or partially polymerized PEGDA monomer.

Given the chemical structure and low thickness of these selective layers, the resultant membranes are expected to be highly permeable. However, this needs to be verified by filtration experiments that demonstrate their performance in more realistic situations. Thus, we next examined the permeation properties of the hydrogel-coated membranes.

Permeation Properties. To characterize how membranes prepared by IIFRP perform in aqueous filtration applications, we performed filtration experiments using a dead-end system.

DOI: 10.1021/acs.chemmater.7b04598
Chem. Mater. XXXX, XXX, XXX−XXX

First, we aimed to understand the effect of IIFRP process parameters such as the UV exposure time on membrane permeance. For this, monomer solution containing 5% v/v PEGDA and 2.5% v/v PEG200 was used to form hydrogel layers by IIFRP at different UV exposure times (4−20 min) on identical support membranes. Deionized water was filtered through the membrane until the flow rate stabilized. Pure water permeance, defined as the water flux through the membrane normalized by the applied pressure difference of 40 psi, was calculated. This permeance was stable over a wide range of transmembrane pressures, up to 60 psi (see Figure S4, Supporting Information). The support membrane was measured to have a water permeance of 1250 ± 60 L h^{-1} m^{-2} bar^{-1}.

Figure 3 shows the water permeances of these hydrogel-coated membranes. Even the membrane prepared with the shortest UV exposure time of 4 min had a substantially lower permeance than the support membrane, 6.2 L h^{-1} m^{-2} bar^{-1}. This indicates the formation of the hydrogel layer. Membranes prepared with 5−20 min UV exposure times also showed substantially lower permeances compared with the support membrane. Longer UV exposure initially led to lower permeance, but the values reached a plateau after 10 min, indicated by the dotted line (B-Spline fitting). A minimum UV exposure time of 4 min was needed for the formation of a uniform hydrogel layer with permeation properties that are distinctly different from the support membrane. Shorter exposure times (1−3 min) lead to membranes with permeances comparable with the support membrane, indicating that a complete hydrogel layer integrated into the support had not yet formed at this time. These results correlate well with and further confirm the morphological results acquired via FESEM (Figure 1). The membrane featuring a thinner hydrogel layer (5 min, Figure 1d) exhibits 1.4 times higher permeance than the ones with thicker layers (20 min, Figure 1f).

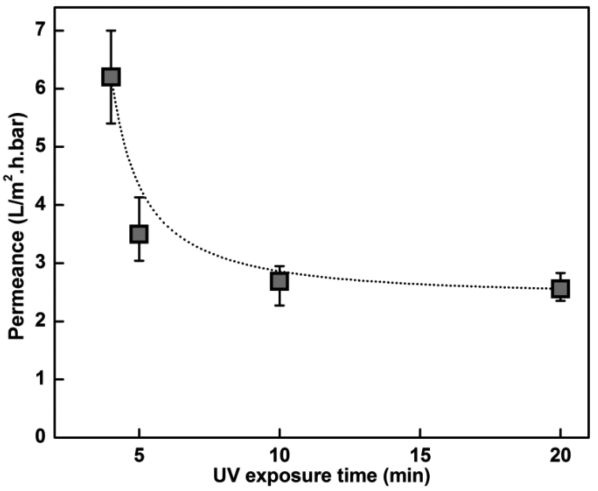

Figure 3. Effect of UV exposure time on membrane permeance; all membranes are prepared with monomer solution containing 5% PEGDA and 2.5% PEG200. Significant difference between the permeance of the support membrane and hydrogel-coated membranes indicates the formation of the hydrogel layer, with permeances depending on UV exposure time.

The error bars shown in Figure 3 represent the maximum and minimum permeance values measured during the test of at least 5 samples for each condition. The narrow range of resultant permeances, indicated by the small error bars, clearly depicts the reproducible, consistent, robust, and reliable nature of our simple IIFRP method.

The permeance range we have achieved in this study is comparable to commercial thin film composite (TFC) membranes with cross-linked selective layers prepared by IP with the largest available pore size. These membranes are tight ultrafiltration (UF) membranes, typically designed for nominal molecular weight cutoff (MWCO) values between 1000 and 3000 Da. For example, according to industrial specification sheets, UF membranes manufactured by GE with nominal MWCOs between 1000 and 3000 Da have permeances between 1.12 and 5.65 L m^{-2} h^{-1} bar^{-1}.[42] It is also significantly higher than free-standing hydrogel membranes reported in the literature, 0.002−0.3 l m^{-2} h^{-1} bar^{-1}.

At this stage, the water permeance of our membrane is lower than values listed for commercial membranes commonly used for bioseparations, such as regenerated cellulose UF membranes.[43] However, as discussed below, the fouling behaviors of hydrogel membranes are significantly different from most commercial membranes, which are prone to severe fouling upon exposure to solutions containing organic macromolecules (e.g., proteins, polysaccharides) and oil.[44−46] The IIFRP method presented here enables the preparation of membranes with highly hydrophilic hydrogel selective layers with excellent antifouling properties. These membranes retain their initial permeance fully even when filtering protein solutions, as demonstrated in the data below. In contrast, commercial membranes, including those made of the relatively hydrophilic regenerated cellulose, often exhibit severe declines in permeance during the filtration of protein solutions due to fouling. For example, even though the Ultracel PLCGC membrane manufactured by EMD Millipore with MWCO of 10 kDa has a higher permeance when tested with pure water, its permeance declines severely during the filtration of protein solutions. Some reported permeances during the filtration of representative protein solutions (bovine skim colostrum whey or surfactin) range between 1.7 and 7 L m^{-2} h^{-1} bar^{-1},[47,48] comparable with the permeances documented for membranes reported here. Similarly high flux decline has also been reported for larger MWCO Ultracel membranes.[49−51] Thus, the exceptional fouling resistance of membranes prepared by IIFRP can enable comparable and more stable membrane permeance during the filtration of protein solutions encountered in bioseparations.

Furthermore, we believe that the IIFRP process has the potential to be tuned and optimized by changing other parameters (e.g., photoinitiator concentration, monomer concentration, additives) to further improve the permeance of resultant membranes. Improved flux can also be achieved by identifying the optimal support membrane for each application. The literature shows that the selection of the support membrane can change the permeance of the TFC membranes by up to an order of magnitude.[52] Therefore, highly competitive and stable permeances can be achieved upon the optimization of the IIFRP process for each targeted bioseparation.

Membrane Selectivity and Protein Rejection. Next, we examined the performance of hydrogel-coated membranes prepared by IIFRP for the filtration of protein solutions in a dead-end filtration setup (Figure 4). For this, different protein solutions were filtered through the hydrogel-coated membranes prepared with a monomer solution of 5% v/v PEGDA and

DOI: 10.1021/acs.chemmater.7b04598
Chem. Mater. XXXX, XXX, XXX−XXX

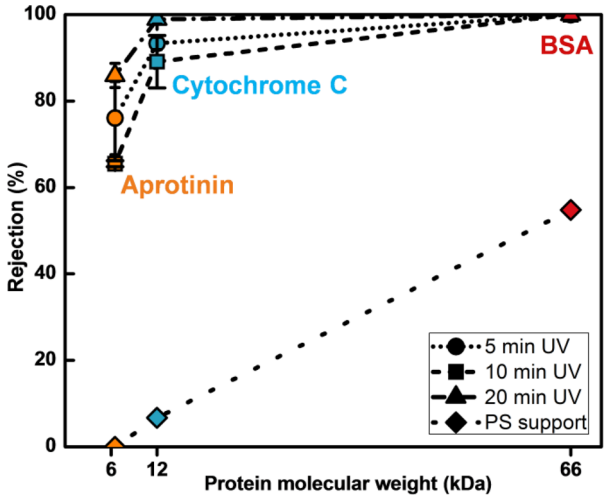

Figure 4. Rejection properties of hydrogel-coated membranes. The PS support membrane shows limited rejection for all three proteins, whereas cross-linked PEGDA-coated membranes prepared by IIFRP reject Cytochrome C and BSA by >90%, indicating a MWCO around 8−10 kDa.

2.5% v/v PEG200 at different UV exposure times (5−20 min). The membranes were first compacted by filtering deionized water for at least 3 h. Three proteins with different molecular weights and hydrodynamic radii (R_H) were tested: Aprotinin (6.5 kDa, $R_H \sim 1.3$ nm), Cytochrome C (12 kDa, $R_H \sim 1.7$ nm), and bovine serum albumin (BSA, 66 kDa, $R_H \sim 3.5$ nm).[53] Each protein was dissolved in phosphate buffered saline (PBS) at a concentration of 100 ppm and filtered through the membrane one at a time. Rejection (R) was calculated by measuring the UV absorbances of feed and permeate at 280 nm for BSA and Aprotinin and 410 nm for Cytochrome C according to

$$R\% = \left(1 - \frac{C_P}{C_F}\right) \times 100$$

where C_F and C_P are the concentration of feed and permeate, respectively.

Figure 4 shows the rejection of these three proteins by the support membrane and three hydrogel-coated membranes prepared by IIFRP using different UV irradiation times. All hydrogel-coated membranes exhibit similar rejection properties, with an effective pore size significantly smaller than the support membrane. For the smallest protein Aprotinin (6.5 kDa), all the membranes prepared by IIFRP show moderate rejection (65−85%). In contrast, Aprotinin passes through the support membrane with no measurable rejection. All three hydrogel-coated membranes show higher rejection (90−99.9%) for the slightly larger Cytochrome C (12 kDa) than the support membrane, which shows only 6% rejection. Finally, for the largest protein, BSA (66 kDa), complete rejection within the detection limit (>99%) was obtained for all the three hydrogel-coated membranes, whereas 55% rejection was observed for the support membrane. This is consistent with a MWCO of about 8−10 kDa for the hydrogel-coated membranes, clearly illustrating the formation of a selective layer that controls membrane selectivity and protein rejection. It is worth noting that the protein rejections remained unchanged upon changing the ionic strength of the solution (Table S1, Supporting Information).

All three hydrogel-coated membranes had similar rejections, within error margins of each other. This suggests that UV exposure time mainly affects hydrogel layer thickness and not the hydrogel mesh size. Importantly, all the consistent protein rejection results with small error bars (indicating the rejection range from minimum 3 membrane samples per condition) confirm minimal defects throughout the membrane area (4.1 cm^2), providing evidence of the reliable and robust nature of IIFRP for preparing membrane selective layers. Furthermore, the hydrogel selective layer shows a much sharper size-based cutoff in comparison to the support membrane.

Since membranes are usually delivered in dry state, we investigated the effect of drying and rehydration on membrane permeance and rejection properties. The membrane was air-dried overnight and soaked in water afterward. Then, membrane permeance and rejection were measured. Both permeance and rejection properties of the membranes remained unchanged after two drying and rehydration cycles. This confirms the absence of any cracks, pore collapse, or defects upon loss of water (Supporting Information).

Effect of Monomer Solution Composition on Membrane Selectivity and Permeance. Membrane selectivity and permeance is affected by various parameters that can be adjusted in the IIFRP process, including the composition of the aqueous monomer solution. These parameters can be used to tune membrane pore size, optimize the process to achieve high permeance while maintaining desired selectivity, and to incorporate desired functional groups in the selective layer for various purposes. For example, the PEGDA concentration in this solution can be changed. Alternatively, other components can be added to this solution. Inert polymers such as low-molecular-weight poly(ethylene glycol) (PEG) can act as porogens by altering the cross-link density and hence mesh size, or create larger-scale voids through PIPS. Comonomers can also alter the mesh size by increasing the distance between cross-links, but also incorporate functional groups in the selective layer. The IIFRP process allows a wide selection of such components; as long as these components are water-soluble, they can be used.

To demonstrate this, we prepared PEGDA hydrogel-coated membranes by IIFRP using different PEGDA concentrations (5−20% v/v) in the monomer solution, and also using PEG200 as an additive at a volume ratio of 2:1 PEGDA:PEG200. The pure water permeance of these membranes, prepared with 5 min UV exposure, was measured in a dead-end filtration system at a transmembrane pressure (TMP) of 40 psi.

Figure 5 shows the change in membrane pure water permeance with varying PEGDA concentration in the monomer solution. When the PEGDA concentration increased from 5% to 10% v/v, membrane permeance decreased by 5 times. The permeance decreased further upon increasing PEGDA content to 20% v/v. This trend could be attributed to the formation of a selective layer with higher polymer content and cross-link density, and therefore a smaller effective pore size of the hydrogel network. These results are consistent with the literature on free-standing PEG hydrogels in that the monomer content directly controls the hydrogel layer cross-link density, which would in turn determine the effective mesh size and MWCO.[54,55] The IIFRP hydrogel-coated membranes also show thicker dry thickness upon increased PEGDA concentration (Figure S5, Supporting Information) due to faster polymerization achieved at higher monomer concentrations,

DOI: 10.1021/acs.chemmater.7b04598
Chem. Mater. XXXX, XXX, XXX−XXX

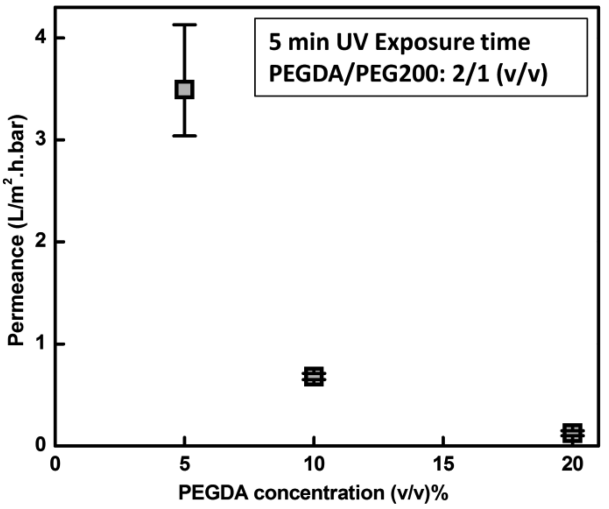

Figure 5. Effect of PEGDA concentration on membrane permeance. Error bars indicate the range of permeances obtained for a minimum of three samples.

and to higher polymer content in the resultant hydrogel layer leading to a thicker film when dried for SEM imaging.

We next examined the effect of different inert additives such as low-molecular-weight PEG (PEG200 and PEG600, with average molar masses of 200 and 600 Da, respectively) on the permeation and rejection properties of membranes prepared by IIFRP of PEGDA (Table 1). For this, we added the PEG oligomers at varying concentrations (0−30% v/v) to the monomer solution and performed IIFRP using a 5 min UV exposure time. The presence of PEG oligomers during the gelation of PEGDA in water is reported to cause phase separation between PEG and PEGDA during photopolymerization, termed polymerization-induced phase separation (PIPS).[54] PEG oligomers are inert porogens that do not polymerize with PEGDA, and are washed away upon rinsing.[56] This leads to the formation of pores or voids.[54,57,58] The presence of voids within the selective layer leads to an increase in the permeance and/or pore size of the resultant membranes, enabling us to tune their separation properties to the desired application.

Table 1 shows the pure water permeances of these membranes, and the rejections of two proteins, BSA and Cytochrome C, as an indicator of their effective pore size. The two top rows of Table 1 show that a small amount of PEG200 (2.5% v/v) increases the permeance by 1.8 times over the hydrogel-coated membrane without the PEG200 while maintaining similar protein rejection properties. Increasing PEG200 content further to 10% v/v increases the membrane permeance to about 3 times the value for the membrane prepared without PEG200, but causes no significant change in rejection. Our hypothesis is that PIPS during this process does not create interconnected large pores, but discrete voids, or cells, similar to those observed in closed-cell foams. The voids are enclosed with continuous hydrogel "walls" within the selective layer, so membrane selectivity is unchanged. However, the enclosed voids do not pose resistance to flow. Hence, the "effective film thickness", or the net thickness that will pose resistance to flow, is lower than the depth polymerization progresses to. This can improve the permeance subsequently, without changing the mesh size of the PEGDA network.[59] As an interesting parallel, recent studies have reported the presence of interspersed voids within the thin polyamide selective layers of RO membranes manufactured by IP method.[31,60] These voids are filled with water during filtration and result in the creation of a shorter diffusion path and thus higher permeance. Our results indicate that a similar mechanism of increased permeance may be at play when PEG200 is used as an additive at low to moderate concentrations, though these results warrant further morphological characterization as a future study. In addition, PIPS may lead to an increase in the fractional free volume of the selective layer by creating voids smaller than the size of the protein within the layer, again leading to a higher permeance without a change in selectivity.

Upon further addition of PEG200 (20% v/v), the permeance decreases, yet similar rejection properties are obtained. This decrease in permeance could be explained by the fact that high amount of PEG200 (δ = 19.1 $MPa^{1/2}$)[61] can increase the solubility of the PI (δ = 24.3 $MPa^{1/2}$, calculated using Molecular Modeling Pro software) in the water phase (δ = 47.9 $MPa^{1/2}$).[62] This may cause some of the PI to partition into the monomer solution before UV exposure, leading the polymerization reaction to no longer occur just at the interface, allowing the hydrogel layer to penetrate into the membrane pores. However, when 30% v/v PEG200 was used in the monomer solution, the resultant permeance was about 3 times the value for the membrane prepared without any PEG200. This was accompanied with a decrease in the rejection of both BSA and Cytochrome C. This is likely due to the formation of interconnected pores by PIPS at this high concentration of PEG200. Inert additives such as PEG oligomers can also interfere with the polymerization reaction when present at high concentrations.[63] This could also have resulted in the observed decrease in protein rejection.

Table 1. Effect of Comonomer/Porogens as Additives in Monomer Solution on Hydrogel-Coated Membranes' Permeance and Rejection Properties[a]

membrane sample	permeance (L m^{-2} h^{-1} bar^{-1})	BSA rejection %	Cytochrome C rejection %
5% PEGDA	1.9 ± 0.3	>99[b]	92.5 ± 1.1
5% PEGDA/2.5% PEG200	3.5 ± 0.5	>99	93.4 ± 2.0
5% PEGDA/10% PEG200	5.9 ± 0.4	>99	96.7 ± 1.3
5% PEGDA/20% PEG200	3.8 ± 1.2	>99	94.9 ± 0.9
5% PEGDA/30% PEG200	6.3 ± 1.6	85 ± 2	71 ± 7
5% PEGDA/30% PEG600	8.1 ± 1.5	70 ± 7	65 ± 9
5% PEGDA/2.5% PEGMEA	2.6 ± 0.7	>99	95.0 ± 0.6
7.5% PEGDA	1.1 ± 0.3	>99	99.5 ± 0.3

[a]Error margins indicate standard deviation from at least three samples. [b]Detection limit.

DOI: 10.1021/acs.chemmater.7b04598
Chem. Mater. XXXX, XXX, XXX−XXX

PEG600 has been documented to create larger pores in cross-linked PEG gels than PEG200 due to PIPS occurring more significantly than with PEG200.[35] However, our results indicate that addition of 10−20% v/v PEG600 leads to similar results as those obtained with similar amounts of PEG200. Similar to PEG200, higher permeance (more than 4 times in comparison to the one without porogen) and lower protein rejections were obtained at 30% v/v PEG600. These changes, however, were more significant than those observed for PEG200. The formation of larger pores by PEG600 can be attributed to either PIPS occurring to a larger extent in comparison to the PEG200 porogen,[35] or to PEG600 inhibiting polymerization to a greater extent than PEG200.[59] This shows that the hydrogel network can be easily tuned using different porogens.

Cross-link density and PIPS can also be influenced by the presence of a monofunctional comonomer such as poly(ethylene glycol) methyl ether acrylate (PEGMEA) mixed with PEGDA in the monomer solution.[39] The results in the two bottom rows of Table 1 show that copolymerization of PEGMEA with PEGDA leads to a higher membrane permeance in comparison with a membrane made with PEGDA only (7.5% v/v). BSA is fully retained by both membranes, whereas the rejection of smaller Cytochrome C decreases somewhat, indicating a slight increase in the effective pore size of the membrane. The replacement of some PEGDA with PEGMEA would decrease the cross-link density in comparison with the membrane containing only PEGDA, leading to this higher mesh size that controls protein selectivity.[19,39] Long pendant chains introduced by the addition of PEGMEA to the hydrogel network can disrupt polymer chain packing and thus decrease cross-link density.[64] Also, PEGMEA with free methoxy chain end-groups decreases the cross-link density by decreasing the fraction of polyfunctional monomers that create cross-links and providing more fractional free volume in the network.[19,39] Unlike PEG porogens, PEGMEA also participates in the polymerization reaction. This increases the effective monomer concentration in solution (compared with, for example, the membrane prepared from 5% PEGDA and 2.5% PEG200) and hence leads to a higher polymer content and lower permeance in comparison with membranes prepared with inert porogens from 5% PEGDA.

Finally, consistently small deviations (i.e., permeance range shown by error bars in Figure 5 and standard deviations in Table 1) were obtained for each condition tested using these additives. This indicates the robustness and reliability of our simple process for forming hydrogel membrane selective layers.

Combined, the results in Figure 5 and Table 1 demonstrate that our robust IIFRP technique yields readily tunable membrane parameters widening the scope for various protein separation applications. Also, while not fully explored in this study, the selective layer can be modified to include many other water-soluble components (e.g., comonomers, porogens, nanomaterials). By carefully tuning the parameters, a hydrogel selective layer can be designed for targeted separations (e.g., charged- or affinity-based separations).

Fouling Resistance. Fouling resistance is crucial for the successful use of membranes.[65] Fouling is a particularly prominent challenge in protein separation applications, because proteins are especially prone to adsorb on the membrane surface and inside the pores.[9,10] This can cause substantial flux decline and cause changes in membrane selectivity due to pore narrowing.[9,11,12] Therefore, it is crucial for newly developed membrane materials to resist fouling to ensure reliable, long-term operation, especially for such high-fouling applications. We thus examined the fouling of hydrogel-coated membranes prepared by IIFRP during the filtration of a protein solution over an extended period of time. For this, we performed a cyclic filtration experiment with 100 ppm BSA solution as a model protein in a cross-flow setup at a TMP of 40 psi and feed flow rate of 135 mL min^{-1}, corresponding to a shear rate of 9.4 s^{-1} over two 6 h periods of protein filtration, between which deionized water was filtered through the membrane for 2 h (Figure 6). Experiments were performed using a round

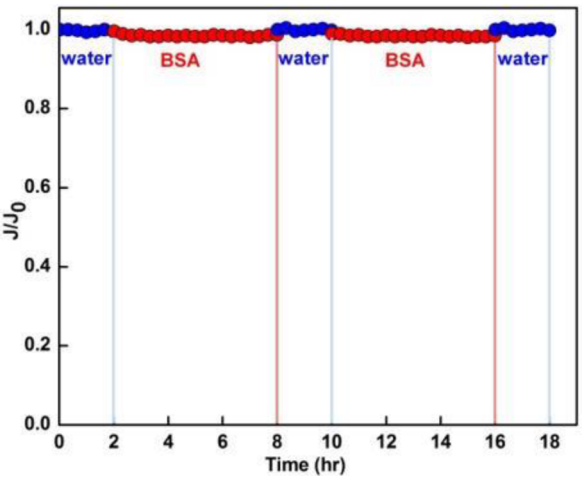

Figure 6. Long-term fouling resistance of hydrogel-coated membrane upon exposure to a model protein (BSA) solution. Tests performed in a cross-flow setup at a TMP of 40 psi; flux is normalized by average initial water flux. The hydrogel-coated membrane is extremely fouling-resistant, suitable for protein purification.

membrane swatch with an effective filtration area of 4.1 cm^2. For the fouling experiment, we chose the membrane prepared with 5% v/v PEGDA and 2.5% v/v PEG200 at UV exposure time of 5 min as an example. This membrane showed high permeance and high rejection for BSA (>99%), so no internal pore fouling was expected, emphasizing the fouling resistance of the hydrogel layer covering the surface.

The membrane was first equilibrated and compacted by filtering deionized (DI) water for 5 h. The initial water flux at the end of this period, termed J_0, was measured to be 12.5 L m^{-2} h^{-1}, corresponding to a permeance of 4.6 L m^{-2} h^{-1} bar^{-1}. Next, BSA solution was filtered through the membrane for 6 h. The membrane initially showed <2% reduction in flux during the filtration of this solution, and no further noticeable decline in flux throughout the 6 h period. It is worth noting that the 2% drop in the flux of protein solution could arise from the osmotic pressure difference caused by the presence of retained solutes in the feed and from concentration polarization rather than an indication of any fouling.[66,67] The lack of further flux decline during operation implies no build-up of foulants occurs on the membrane surface, due to the adsorption of proteins or due to cake formation.[68,69] Next, to test the reversibility of this minor decline in flux and confirm its cause, the feed was switched to DI water for two hours. The membrane immediately returned to its initial flux without the need for backwashing or chemical cleaning, clearly indicating excellent resistance to fouling by this protein. Comparable results were achieved during the second protein filtration cycle. No fouling was observed in this second

DOI: 10.1021/acs.chemmater.7b04598
Chem. Mater. XXXX, XXX, XXX−XXX

protein filtration cycle either. BSA molecules were retained by >99%. The membrane immediately returned to its initial water flux upon water filtration afterward. This result clearly illustrates the excellent antifouling property and robustness of our hydrogel-coated membrane over extended exposure to protein solutions. In contrast, commercial UF membranes used in protein separations (e.g., made of PS) are known to foul extensively and immediately upon exposure to protein solutions, often leading to severe flux decline during the filtration of the solution, as well as flux declines of more than 50% that cannot be reversed even by more complex physical cleaning procedures compared with those used in this experiment.[12,16,70] The excellent fouling resistance demonstrated in this experiment illustrates the potential of IIFRP to prepare highly fouling-resistant membranes for protein separation.

■ CONCLUSION

This report is the first demonstration of a new, robust interfacial polymerization-based technique, IIFRP, to manufacture membranes with ultrathin hydrogel selective layers, their key performance parameters relevant to protein purification and separation applications. As an initial demonstration of this technique, this study focused on membranes with cross-linked PEGDA selective layers, prepared using varying UV irradiation times and with comonomers or inert additives. The formation of uniform hydrogel layers as thin as <100 nm was documented at different UV exposure times using FESEM, and confirmed via FTIR. Water filtration experiments showed that membranes prepared by IIFRP exhibited reliable and consistent performance. Uniform selective layers with complete coverage were formed at a UV irradiation time of 4−5 min, with longer exposures leading to thicker selective layers and lower permeance without any significant shift in selectivity. The filtration of proteins with different molecular weights revealed the formation of defect-free and uniform selective layers, indicated by complete rejection of higher-molecular-weight solutes. Initial membranes prepared with solutions containing 5% v/v PEGDA and 2.5% v/v PEG200 had a MWCO of around 8−10 kDa. The permeance can be further improved, and MWCO can be adjusted, by adjusting simple fabrication parameters such as the monomer concentration or by the incorporation of comonomers or inert additives that act as porogens in the monomer solution. Lastly, extended protein filtration experiments showed that the membranes exhibit excellent antifouling properties and stability for protein purification. Taken together, these results indicate that the newly described IIFRP is a facile and robust fabrication strategy to manufacture membranes with uniform and defect-free hydrogel selective layers with tunable protein filtration properties. Unlike common single-phase polymerization methods used to prepare membranes with hydrogel selective layers, IIFRP allows for the formation of ultrathin hydrogel layers. Furthermore, IIFRP leads to uniform selective layers due to the formation of the hydrogel layer at an interface spanning the surface of the support, minimizing defects. We envision that this novel fabrication method can open up promising routes for industrial-scale fabrication of ultrathin hydrogel selective layers. Furthermore, IIFRP can be readily extended to the fabrication of hydrogels with additional functionalities via incorporation of different comonomers (e.g., charged monomers, zwitterions, etc.) in a reliable and reproducible manner for a variety of applications.

■ EXPERIMENTAL METHODS

Materials. Poly(ethylene glycol) diacrylate (PEGDA, average M_n 700 Da), poly(ethylene glycol) methyl ether acrylate (PEGMEA, average M_n 480 Da), poly(ethylene glycol) (PEG, average M_n 200 or 600 Da), 2-hydroxy-2-methylpropiophenone also known as Darocur 1173 (photoinitiator, PI), and bovine serum albumin (BSA) were purchased from Sigma-Aldrich (St. Louis, MO). *n*-Hexadecane (99%) was purchased from ACROS Organics. Cytochrome C, equine heart, +90%, and Aprotinin, from bovine lung, were purchased from Alfa Aesar (Ward Hill, MA). Phosphate buffered saline (PBS) packs (0.1 M sodium phosphate, 0.15 M sodium chloride, pH 7.2) were purchased from Thermo Scientific (Rockford, IL). Reagent alcohol was obtained from VWR (West Chester, PA). Ultrapure deionized water generated by Biolab 3300 RO, a building-wide RO/DI water purification unit by Mar Cor Purification, was used for all experiments. All the chemicals were analytical grade, and used without further purification. Polysulfone (PS35, 20 kDa) ultrafiltration membranes purchased from Nanostone Water, Inc. (Oceanside, CA) were used as the support membrane to provide mechanical stability.

Fabrication of Ultrathin Hydrogel Layer. The support membrane (Polysulfone, PS, Nanostone) was first washed with ethanol, dried, and then taped along all edges onto a glass plate. An aqueous solution containing 5−20% v/v PEGDA (700 g mol^{-1}), with or without additives (PEG200, PEG600, or PEGMEA), was poured on the support membrane. The support membrane was equilibrated with this aqueous monomer solution for 3 min to provide enough time for monomers, comonomers, and porogens to diffuse into the pores. The penetration of PEGDA into PS helps further stability of the coating layer on PS. The aqueous solution was then poured out, and the membrane surface was gently dabbed using a filter paper to remove any residual droplets. A solution of 0.1% v/v of oil-soluble PI (Darocur) in *n*-hexadecane was poured on the membrane surface. The membrane surface was covered with a glass plate to prevent initiation from PS support membrane.[37,38] Subsequently, the membrane was exposed to 365 nm UV light with an 8 W hand-held UV lamp (Spectronics Corp., Westbury, NY) for varying times (1−20 min). The excess solution covering the membrane was then poured out, and the membrane surface was washed with a water/ethanol mixture 1:1 ratio several times and kept in DI water overnight to ensure the complete removal of unreacted monomer, additives, initiator, and hexadecane.

Field-Emission Scanning Electron Microscopy (FESEM). The microstructure of the membrane was characterized by Field-emission scanning electron microscopy (Supra 55) at 4 kV and 7 mm working distance. Dried membranes were frozen in liquid nitrogen and cut with a razor blade for cross-sectional imaging. Samples were sputter-coated (Cressington 108 manual, Ted Pella Inc., CA) with Au/Pd (60/40) in an argon atmosphere.

Attenuated Total Internal Reflectance−Fourier Transform Infrared (ATR−FTIR). ATR−FTIR spectra of membranes were collected using a FTIR-6200 spectrophotometer (JASCO Corp, Tokyo, Japan) over the range 4000−600 cm^{-1} at a 2 cm^{-1} resolution. Prior to analysis, membranes were air-dried for 24 h.

Membrane Performance. Filtration experiments were performed using an Amicon 8010 dead-end stirred cell (Millipore) with a cell volume of 10 mL and an effective filtration area of 4.1 cm^2 attached to a 1 gal reservoir. The cell was stirred at 500 rpm. Tests were conducted at an applied transmembrane pressure (TMP) of 40 psi. Water flow rate through the membranes was measured by collecting the permeate in a container placed on a scale (Ohaus Scout Pro) connected to a computer and recording the increase in permeate weight over time. The membrane permeance (L_p) was calculated by normalizing flux (J), defined as the water flow rate divided by active membrane area, with applied transmembrane pressure (ΔP):

$$L_p = \frac{J}{\Delta P}$$

Membrane performance in protein filtration was studied by filtering solutions of a series of proteins with different sizes at a concentration of 100 ppm in PBS buffer one at a time. The first 1 mL of filtrate was

DOI: 10.1021/acs.chemmater.7b04598
Chem. Mater. XXXX, XXX, XXX−XXX

discarded, and the subsequent 1 mL was collected. The concentration of protein in this filtrate was measured using UV−vis spectroscopy (Thermo Scientific Genesys 10S spectrometer, Waltham, MA) at 285 nm for BSA and Aprotinin and 410 for Cytochrome C. Protein rejection was calculated according to

$$R\% = \left(1 - \frac{C_P}{C_F}\right) \times 100$$

where R is the solute rejection, and C_F and C_P are the concentration of feed (100 ppm) and permeate, respectively. Membranes were washed (soaked in DI water, and DI water was filtered through overnight) before subsequent protein filtration experiments. No significant shift in water permeance was noted between protein filtration experiments.

The fouling properties of the membrane were investigated in a cross-flow system with a flat-frame membrane module (Sterlitech CF016A, Kent, WA) integrated with a KrosFlo Research II TFF System (Spectrum Laboratories, Inc., Compton, CA). The CF016 cell, with an as-manufactured effective membrane area of 20.6 cm^2 and a channel depth of 2.3 mm, was fitted with an impermeable plastic mask that allowed the installation of round membrane swatches with an effective filtration area of 4.1 cm^2. Experiments were performed at transmembrane pressure (TMP) of 40 psi and feed flow rate of 135 mL min^{-1}, corresponding to a shear rate of 9.4 s^{-1} and a Reynolds number of 120, indicating laminar flow. This value was selected based on the literature that reports more severe irreversible fouling occurring at low *Re* numbers.[71−73]

■ ASSOCIATED CONTENT

Supporting Information

The Supporting Information is available free of charge on the ACS Publications website at DOI: 10.1021/acs.chemmater.7b04598.

Control experiment with monomer and initiator in single aqueous phase, and effect of monomer solution concentration on hydrogel layer thickness (PDF)

■ AUTHOR INFORMATION

Corresponding Author

*E-mail: Ayse.Asatekin@tufts.edu.

ORCID

Ayse Asatekin: 0000-0002-4704-1542

Notes

The authors declare no competing financial interest.

■ ACKNOWLEDGMENTS

We gratefully acknowledge financial support from Tufts University, the Tufts Collaborates program, and the National Science Foundation (NSF) under Grants CBET-1703549 and CBET-1553661. FESEM imaging was performed at the Center for Nanoscale Systems (CNS), a member of the National Nanotechnology Infrastructure Network (NNIN), which is supported by the National Science Foundation under NSF Award ECS-0335765. CNS is part of Harvard University.

■ REFERENCES

(1) Labrou, N. E. Protein Purification: An Overview. *Methods Mol. Biol.* **2014**, *1129*, 3−10.

(2) Hettiarachchy, N.; Sato, K.; Marshall, M.; Kannan, A. *Food Proteins and Peptides: Chemistry, Functionality, Interactions, and Commercialization*; CRC Press: Taylor & Francis Group: FL, 2016.

(3) van Reis, R.; Zydney, A. Membrane separations in biotechnology. *Curr. Opin. Biotechnol.* **2001**, *12* (2), 208−211.

(4) Charcosset, C. Membrane processes in biotechnology: An overview. *Biotechnol. Adv.* **2006**, *24* (5), 482−492.

(5) Zhao, Y. H.; Wee, K. H.; Bai, R. B. A Novel Electrolyte-Responsive Membrane with Tunable Permeation Selectivity for Protein Purification. *ACS Appl. Mater. Interfaces* **2010**, *2* (1), 203−211.

(6) Huang, R.; Kostanski, L. K.; Filipe, C. D. M.; Ghosh, R. Environment-responsive hydrogel-based ultrafiltration membranes for protein bioseparation. *J. Membr. Sci.* **2009**, *336* (1−2), 42−49.

(7) Li, Q.; Bi, Q. Y.; Lin, H. H.; Bian, L. X.; Wang, X. L. A novel ultrafiltration (UF) membrane with controllable selectivity for protein separation. *J. Membr. Sci.* **2013**, *427*, 155−167.

(8) Adrus, N.; Ulbricht, M. Novel hydrogel pore-filled composite membranes with tunable and temperature-responsive size-selectivity. *J. Mater. Chem.* **2012**, *22* (7), 3088−3098.

(9) Nilsson, J. L. Protein Fouling of Uf Membranes - Causes and Consequences. *J. Membr. Sci.* **1990**, *52* (2), 121−142.

(10) Tang, C. Y. Y.; Chong, T. H.; Fane, A. G. Colloidal interactions and fouling of NF and RO membranes: A review. *Adv. Colloid Interface Sci.* **2011**, *164* (1−2), 126−143.

(11) Kang, S.; Asatekin, A.; Mayes, A. M.; Elimelech, M. Protein antifouling mechanisms of PAN UF membranes incorporating PAN-g-PEO additive. *J. Membr. Sci.* **2007**, *296* (1−2), 42−50.

(12) Marshall, A. D.; Munro, P. A.; Tragardh, G. The Effect of Protein Fouling in Microfiltration and Ultrafiltration on Permeate Flux, Protein Retention and Selectivity - a Literature-Review. *Desalination* **1993**, *91* (1), 65−108.

(13) Yang, Q.; Adrus, N.; Tomicki, F.; Ulbricht, M. Composites of functional polymeric hydrogels and porous membranes. *J. Mater. Chem.* **2011**, *21* (9), 2783−2811.

(14) Ju, H.; McCloskey, B. D.; Sagle, A. C.; Kusuma, V. A.; Freeman, B. D. Preparation and characterization of crosslinked poly(ethylene glycol) diacrylate hydrogels as fouling-resistant membrane coating materials. *J. Membr. Sci.* **2009**, *330* (1−2), 180−188.

(15) Andrade, J. D.; Hlady, V.; Jeon, S. I. Poly(ethylene oxide) and protein resistance - Principles, problems, and possibilities. *Adv. Chem. Ser.* **1996**, *248*, 51−59.

(16) Ju, H.; McCloskey, B. D.; Sagle, A. C.; Wu, Y. H.; Kusuma, V. A.; Freeman, B. D. Crosslinked poly(ethylene oxide) fouling resistant coating materials for oil/water separation. *J. Membr. Sci.* **2008**, *307* (2), 260−267.

(17) Kang, G. D.; Cao, Y. M.; Zhao, H. Y.; Yuan, Q. Preparation and characterization of crosslinked poly(ethylene glycol) diacrylate membranes with excellent antifouling and solvent-resistant properties. *J. Membr. Sci.* **2008**, *318* (1−2), 227−232.

(18) Sagle, A. C.; Van Wagner, E. M.; Ju, H.; McCloskey, B. D.; Freeman, B. D.; Sharma, M. M. PEG-coated reverse osmosis membranes: Desalination properties and fouling resistance. *J. Membr. Sci.* **2009**, *340* (1−2), 92−108.

(19) Sagle, A. C.; Ju, H.; Freeman, B. D.; Sharma, M. M. PEG-based hydrogel membrane coatings. *Polymer* **2009**, *50* (3), 756−766.

(20) Wu, Y. H.; Park, H. B.; Kai, T.; Freeman, B. D.; Kalika, D. S. Water uptake, transport and structure characterization in poly-(ethylene glycol) diacrylate hydrogels. *J. Membr. Sci.* **2010**, *347* (1−2), 197−208.

(21) van Rijn, P.; Tutus, M.; Kathrein, C.; Zhu, L. L.; Wessling, M.; Schwaneberg, U.; Boker, A. Challenges and advances in the field of self-assembled membranes. *Chem. Soc. Rev.* **2013**, *42* (16), 6578−6592.

(22) Nam, K. T.; Kim, D. W.; Yoo, P. J.; Chiang, C. Y.; Meethong, N.; Hammond, P. T.; Chiang, Y. M.; Belcher, A. M. Virus-enabled synthesis and assembly of nanowires for lithium ion battery electrodes. *Science* **2006**, *312* (5775), 885−888.

(23) Allen, M.; Willits, D.; Mosolf, J.; Young, M.; Douglas, T. Protein cage constrained synthesis of ferrimagnetic iron oxide nanoparticles. *Adv. Mater.* **2002**, *14* (21), 1562−1565.

(24) Bhattacharya, A.; Misra, B. N. Grafting: a versatile means to modify polymers - Techniques, factors and applications. *Prog. Polym. Sci.* **2004**, *29* (8), 767−814.

(25) Carroll, T.; Booker, N. A.; Meier-Haack, J. Polyelectrolyte-grafted microfiltration membranes to control fouling by natural organic matter in drinking water. *J. Membr. Sci.* **2002**, *203* (1−2), 3−13.

DOI: 10.1021/acs.chemmater.7b04598
Chem. Mater. XXXX, XXX, XXX−XXX

(26) La, Y. H.; McCloskey, B. D.; Sooriyakumaran, R.; Vora, A.; Freeman, B.; Nassar, M.; Hedrick, J.; Nelson, A.; Allen, R. Bifunctional hydrogel coatings for water purification membranes: Improved fouling resistance and antimicrobial activity. *J. Membr. Sci.* **2011**, *372* (1−2), 285−291.
(27) Lin, H. Q.; Van Wagner, E.; Freeman, B. D.; Toy, L. G.; Gupta, R. P. Plasticization-enhanced hydrogen purification using polymeric membranes. *Science* **2006**, *311* (5761), 639−642.
(28) Lin, H. Q.; Kai, T.; Freeman, B. D.; Kalakkunnath, S.; Kalika, D. S. The effect of cross-linking on gas permeability in cross-linked poly(ethylene glycol diacrylate). *Macromolecules* **2005**, *38* (20), 8381−8393.
(29) Cadotte, J. E. *Reverse osmosis membrane*. U.S. Patent 3,926,798 A, December, 1975.
(30) Cadotte, J. E. *Interfacially synthesized reverse osmosis membrane*. U.S. Patent 4,277,344 A, July, 1981.
(31) Lin, L.; Lopez, R.; Ramon, G. Z.; Coronell, O. Investigating the void structure of the polyamide active layers of thin-film composite membranes. *J. Membr. Sci.* **2016**, *497*, 365−376.
(32) Lin, L.; Feng, C. C.; Lopez, R.; Coronell, O. Identifying facile and accurate methods to measure the thickness of the active layers of thin-film composite membranes - A comparison of seven characterization techniques. *J. Membr. Sci.* **2016**, *498*, 167−179.
(33) Soroush, A.; Barzin, J.; Barikani, M.; Fathizadeh, M. Interfacially polymerized polyamide thin film composite membranes: Preparation, characterization and performance evaluation. *Desalination* **2012**, *287*, 310−316.
(34) Appleyard, D. C.; Chapin, S. C.; Doyle, P. S. Multiplexed Protein Quantification with Barcoded Hydrogel Microparticles. *Anal. Chem.* **2011**, *83* (1), 193−199.
(35) Choi, N. W.; Kim, J.; Chapin, S. C.; Duong, T.; Donohue, E.; Pandey, P.; Broom, W.; Hill, W. A.; Doyle, P. S. Multiplexed Detection of mRNA Using Porosity-Tuned Hydrogel Microparticles. *Anal. Chem.* **2012**, *84* (21), 9370−9378.
(36) Yang, C. X.; Choi, C. H.; Lee, C. S.; Yi, H. M. A Facile Synthesis-Fabrication Strategy for Integration of Catalytically Active Viral-Palladium Nanostructures into Polymeric Hydrogel Microparticles via Replica Molding. *ACS Nano* **2013**, *7* (6), 5032−5044.
(37) Yamagishi, H.; Crivello, J. V.; Belfort, G. Development of a Novel Photochemical Technique for Modifying Poly(Arylsulfone) Ultrafiltration Membranes. *J. Membr. Sci.* **1995**, *105* (3), 237−247.
(38) Pieracci, J.; Crivello, J. V.; Belfort, G. Increasing membrane permeability of UV-modified poly(ether sulfone) ultrafiltration membranes. *J. Membr. Sci.* **2002**, *202* (1−2), 1−16.
(39) Wu, Y. H.; Park, H. B.; Kai, T.; Freeman, B. D.; Kalika, D. S. Water uptake, transport and structure characterization in poly(ethylene glycol) diacrylate hydrogels. *J. Membr. Sci.* **2010**, *347* (1−2), 197−208.
(40) Peter, M.; Tayalia, P. An alternative technique for patterning cells on poly(ethylene glycol) diacrylate hydrogels. *RSC Adv.* **2016**, *6* (47), 40878−40885.
(41) Xiao, Y. H.; He, L.; Che, J. F. An effective approach for the fabrication of reinforced composite hydrogel engineered with SWNTs, polypyrrole and PEGDA hydrogel. *J. Mater. Chem.* **2012**, *22* (16), 8076−8082.
(42) https://www.sterlitech.com/flat-sheet-membranes-specifications.html.
(43) https://www.lenntech.com/Data-sheets/Millipore-Ultrafiltration-Membranes-L.pdf.
(44) Van der Bruggen, B.; Vandecasteele, C.; Van Gestel, T.; Doyen, W.; Leysen, R. A review of pressure-driven membrane processes in wastewater treatment and drinking water production. *Environ. Prog.* **2003**, *22* (1), 46−56.
(45) Sadeghi, I.; Aroujalian, A.; Raisi, A.; Dabir, B.; Fathizadeh, M. Surface modification of polyethersulfone ultrafiltration membranes by corona air plasma for separation of oil/water emulsions. *J. Membr. Sci.* **2013**, *430*, 24−36.
(46) Sadeghi, I.; Aroujalian, A.; Raisi, A.; Fathizadeh, M.; Dabir, B. Effect of solvent, hydrophilic additives and corona treatment on performance of polyethersulfone UF membranes for oil/water separation. *Procedia Eng.* **2012**, *44*, 1539−1541.
(47) Lu, R. R.; Xu, S. Y.; Wang, Z.; Yang, R. J. Isolation of lactoferrin from bovine colostrum by ultrafiltration coupled with strong cation exchange chromatography on a production scale. *J. Membr. Sci.* **2007**, *297* (1−2), 152−161.
(48) Isa, M. H. M.; Coraglia, D. E.; Frazier, R. A.; Jauregi, P. Recovery and purification of surfactin from fermentation broth by a two-step ultrafiltration process. *J. Membr. Sci.* **2007**, *296* (1−2), 51−57.
(49) Kwon, B.; Molek, J.; Zydney, A. L. Ultrafiltration of PEGylated proteins: Fouling and concentration polarization effects. *J. Membr. Sci.* **2008**, *319* (1−2), 206−213.
(50) Lim, Y. P.; Mohammad, A. W. Effect of solution chemistry on flux decline during high concentration protein ultrafiltration through a hydrophilic membrane. *Chem. Eng. J.* **2010**, *159* (1−3), 91−97.
(51) Jermann, D.; Pronk, W.; Boller, M.; Schafer, A. I. The role of NOM fouling for the retention of estradiol and ibuprofen during ultrafiltration. *J. Membr. Sci.* **2009**, *329* (1−2), 75−84.
(52) Ghosh, A. K.; Hoek, E. M. V. Impacts of support membrane structure and chemistry on polyamide-polysulfone interfacial composite membranes. *J. Membr. Sci.* **2009**, *336* (1−2), 140−148.
(53) Talmard, C.; Guilloreau, L.; Coppel, Y.; Mazarguil, H.; Faller, P. Amyloid-beta peptide forms monomeric complexes with Cu-II and Zn-II prior to aggregation. *ChemBioChem* **2007**, *8* (2), 163−165.
(54) Jung, S.; Yi, H. Facile Micromolding-Based Fabrication of Biopolymeric-Synthetic Hydrogel Microspheres with Controlled Structures for Improved Protein Conjugation. *Chem. Mater.* **2015**, *27* (11), 3988−3998.
(55) Jung, S.; Abel, J. H.; Starger, J. L.; Yi, H. Porosity-Tuned Chitosan-Polyacrylamide Hydrogel Microspheres for Improved Protein Conjugation. *Biomacromolecules* **2016**, *17* (7), 2427−2436.
(56) Le Goff, G. C.; Srinivas, R. L.; Hill, W. A.; Doyle, P. S. Hydrogel microparticles for biosensing. *Eur. Polym. J.* **2015**, *72*, 386−412.
(57) Dusek, K. Phase Separation in Ternary Systems Induced by Crosslinking. *Chem. Zvesti* **1971**, *25* (3), 184−189.
(58) Boots, H. M. J.; Kloosterboer, J. G.; Serbutoviez, C.; Touwslager, F. J. Polymerization-induced phase separation 0.1. Conversion-phase diagrams. *Macromolecules* **1996**, *29* (24), 7683−7689.
(59) Lee, A. G.; Arena, C. P.; Beebe, D. J.; Palecek, S. P. Development of Macroporous Poly(ethylene glycol) Hydrogel Arrays within Microfluidic Channels. *Biomacromolecules* **2010**, *11* (12), 3316−3324.
(60) Wong, M. C. Y.; Lin, L.; Coronell, O.; Hoek, E. M. V.; Ramon, G. Z. Impact of liquid-filled voids within the active layer on transport through thin-film composite membranes. *J. Membr. Sci.* **2016**, *500*, 124−135.
(61) Li, M. G.; Humayun, M.; Hughes, B.; Kozinski, J. A.; Hwang, D. K. A microfluidic approach for the synthesis and assembly of multi-scale porous membranes. *RSC Adv.* **2015**, *5* (121), 100024−100029.
(62) Zeng, W.; Du, Y.; Xue, Y.; Frisch, H. Solubility Parameters. In *Physical Properties of Polymers Handbook*; Mark, J., Ed.; Springer: NY, 2007; pp 289−303.
(63) Pregibon, D. C.; Doyle, P. S. Optimization of Encoded Hydrogel Particles for Nucleic Acid Quantification. *Anal. Chem.* **2009**, *81* (12), 4873−4881.
(64) Stevens, M. P. In *Polymer Chemistry: An Introduction*; Oxford University Press: NewYork, 1998; pp 70−74.
(65) Guo, W. S.; Ngo, H. H.; Li, J. X. A mini-review on membrane fouling. *Bioresour. Technol.* **2012**, *122*, 27−34.
(66) Schafer, A. I. *Natural Organics Removal Using Membranes: Principles, Performance, and Cost*; CRC Press: Boca Raton, FL, 2001.
(67) Fathizadeh, M.; Tien, H. N.; Khivantsev, K.; Song, Z.; Zhou, F.; Yu, M. Polyamide/nitrogen-doped Graphene Oxide Quantum Dots (N-GOQD) Thin Film Nanocomposite Reverse Osmosis Membranes for High Flux Desalination. *Desalination* **2017**, 10.1016/j.desal.2017.07.014.

DOI: 10.1021/acs.chemmater.7b04598
Chem. Mater. XXXX, XXX, XXX−XXX

(68) Vandenberg, G. B.; Smolders, C. A. Flux Decline in Ultrafiltration Processes. *Desalination* **1990**, *77* (1−3), 101−133.
(69) Palacio, L.; Ho, C. C.; Zydney, A. L. Application of a pore-blockage - Cake-filtration model to protein fouling during micro-filtration. *Biotechnol. Bioeng.* **2002**, *79* (3), 260−270.
(70) Matthiasson, E. The Role of Macromolecular Adsorption in Fouling of Ultrafiltration Membranes. *J. Membr. Sci.* **1983**, *16* (Dec), 23−36.
(71) Culfaz, P. Z.; Haddad, M.; Wessling, M.; Lammertink, R. G. H. Fouling behavior of microstructured hollow fibers in cross-flow filtrations: Critical flux determination and direct visual observation of particle deposition. *J. Membr. Sci.* **2011**, *372* (1−2), 210−218.
(72) Razi, B.; Aroujalian, A.; Fathizadeh, M. Modeling of fouling layer deposition in cross-flow microfiltration during tomato juice clarification. *Food Bioprod. Process.* **2012**, *90* (C4), 841−848.
(73) Rezaei, H.; Ashtiani, F. Z.; Fouladitajar, A. Fouling Behavior and Performance of Microfiltration Membranes for Whey Treatment in Steady and Unsteady-State Conditions. *Braz. J. Chem. Eng.* **2014**, *31* (2), 503−518.

DOI: 10.1021/acs.chemmater.7b04598
Chem. Mater. XXXX, XXX, XXX−XXX